A Wireless Narrowband Imaging Chip for Capsule Endoscope

Lan-Rong Dung, *Member, IEEE*, and Yin-Yi Wu

***Abstract*—This paper presents a dual-mode capsule gastrointestinal endoscope device. An endoscope combined with a narrowband image (NBI), has been shown to be a superior diagnostic tool for early stage tissue neoplasms detection. Nevertheless, a wireless capsule endoscope with the narrowband imaging technology has not been presented in the market up to now. The narrowband image acquisition and power dissipation reduction are the main challenges of NBI capsule endoscope. In this paper, we present the first narrowband imaging capsule endoscope that can assist clinical doctors to effectively diagnose early gastrointestinal cancers, profited from our dedicated dual-mode complementary metal–oxide semiconductor (CMOS) sensor. The dedicated dual-mode CMOS sensor can offer white-light and narrowband images. Implementation results show that the proposed 512 $\times$ 512 CMOS sensor consumes only 2 mA at a 3-V power supply. The average current of the NBI capsule with an 8-Mb/s RF transmitter is nearly 7 $\sim$ 8 mA that can continuously work for 6 $\sim$ 8 h with two 1.5-V 80-mAh button batteries while the frame rate is 2 fps. Experimental results on backside mucosa of a human tongue and pig's small intestine showed that the wireless NBI capsule endoscope can significantly improve the image quality, compared with a commercial-of-the-shelf capsule endoscope for gastrointestinal tract diagnosis.**

***Index Terms*—Capsule endoscope, complementary metal–oxide semiconductor (CMOS) sensor, gastrointestinal image, narrowband image (NBI).**

I. Introduction

THIS PAPER presents a dual-mode wireless capsule endoscope that features visible and narrowband image acquisition. These days, the early detection and treatment of digestive tract cancers has become an important issue in the field of digestive medicine. Although numerous gastrointestinal endoscopes can travel through the entire alimentary canal, the detection of early cancer during the routine endoscopic examination is still a difficult job. Since the lesions in the early stage are relatively asymptomatic, effective screening methods that would detect an earlier lesion would be of great benefit to patients.

An early pathological change of these tissue neoplasms often has a significant increment in microvessel density. This results in morphologic changes of microvessels in the superficial neoplasm. Capillary patterns beneath the epithelium in these regions will also look different from the surrounding area. Thererfore, the chromoendoscopy, magnify endoscopy, endoscopic ultrasonography, and narrowband imaging (NBI) endoscopy have been developed by using this property. The chromoendoscopy uses a biocompatible dye to enhance the image of capillary patterns; however, to achieve complete and uniform coating of dyes is very difficult and its maintenance cost is notoriously high. The magnify endoscopy can also examine the structure pattern of mucosa by using dye to improve image contrast. Nevertheless, the proper field of vision is hard to locate by the magnify endoscopy for its laborious operation. To overcome these drawbacks of traditional endoscope, K. Gono *et al.* proposed the narrowband image technology [1]–[3]. The NBI is an innovative optical technology using the center wavelengths of 415 nm and 540 nm to clearly visualize the microvascular structure of the organ surface, because 415-nm and 540-nm lights can be absorbed by hemoglobin [1]. Due to the mulitple scattering effect in tissue, the 415-nm light cannot reach the depth where the vessel images can be developed by the 540-nm light. Therefore, the NBI system applies the 415-nm light and 540-nm light to produce images of vessels at superficial mucosal and submucosal layers. From their images of the backside mucosa of human tongue exposed to different center wavelengths of narrowband light, we can learn that the vessel images change greatly according to the center wavelength. Many investigations have been reported on the diagnosis of the head and neck region, bronchus, esophagus, stomach, colon, and early gastric cancer [4], [5] by using NBI technology on the basis of the vascular irregularities.

These days, the gastrointestinal endoscopy, combined with NBI, has been popularly used because it is less invasive, and capable of early stage tissue neoplasms detection. However, there is no NBI technology being applied for the wireless capsule endoscope (CE) [6]–[10]. As mentioned in [11], a wireless capsule endoscope is a highly effective means of examining the entire small bowel. Its clinical use as a diagnostic tool in patients with obscure GI bleeding (OGIB) has been proven in several prospective trials. Nevertheless, the reliability of CE is challenged by [12] in the investigation of OGIB. We believe that the NBI capsule endoscope could be a new and reliable diagnostic tool for detection of early gastrointestinal disease, such as obscure GI bleeding [13].

The proposed NBI capsule endoscope is composed of a narrowband light-emitting diode (LED) light source, a 512 $\times$ 512 dual-mode CMOS image sensor, and an 8 Mb/s RF transmitter. The image sensor associated with the light source can acquire visible and narrowband images during the period of treatment.

Manuscript received April 15, 2010; revised August 08, 2010; accepted September 06, 2010. Date of publication November 11, 2010; date of current version November 24, 2010. This work was supported in part by the National Science Council, R.O.C., under Grant NSC 98-2221-E-009-138 and in part by the Chung-Shan Institute of Science and Technology, Taiwan. This paper was recommended by Associate Editor G. Yuan.

The authors are with the Department of Electrical Engineering, National Chiao Tung University, Hsinchu 30010, Taiwan (e-mail: lennon@faculty.nctu.edu.tw).

Color versions of one or more of the figures in this paper are available online at http://ieeexplore.ieee.org.

Digital Object Identifier 10.1109/TBCAS.2010.2079932

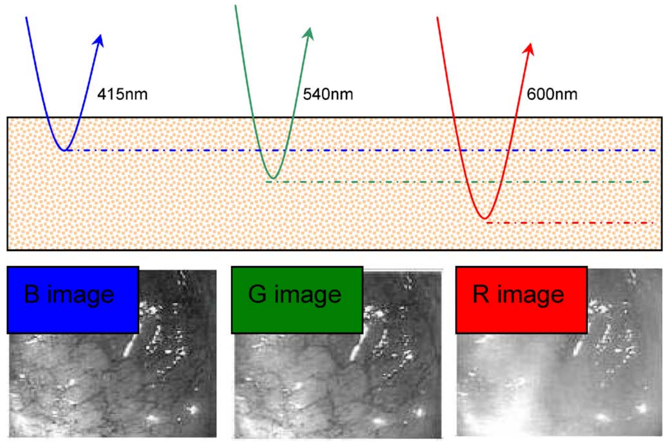

Fig. 1. Principle of NBI (from Olympus Corporation, Japan).

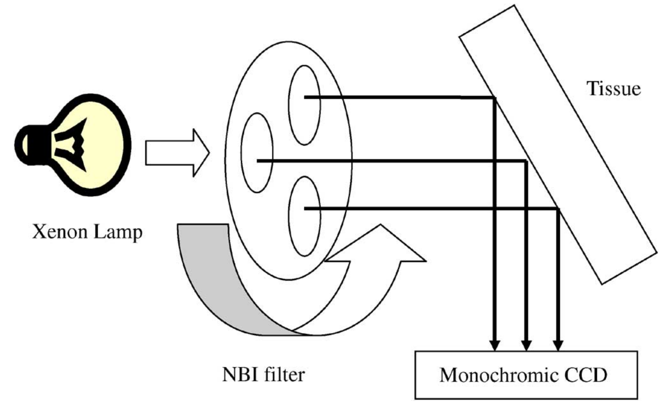

Fig. 2. Configuration of Olympus NBI endoscope system.

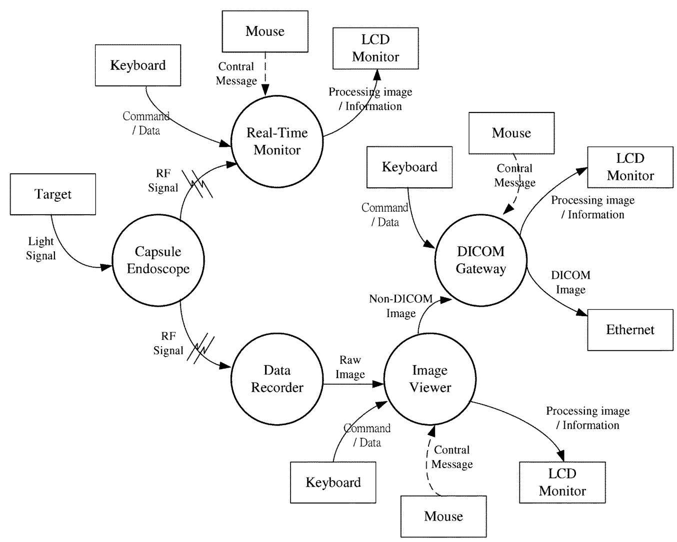

Fig. 3. System description of the wireless NBI capsule endoscope.

The presented dual-mode image sensor acquires one narrowband image and one visible image per second under inter illumination mode. In intra illumination mode, visible and narrowband image are both acquired at a frame rate of 2 frames/s. The sensor consumes only 2 mA at a 3-V power supply. Implementation results show that the NBI capsule endoscope can work about 6 $\sim$ 8 h at 2 frames/s with two button batteries.

The organization of this paper is as follows. Section II introduces the narrowband image and the proposed architecture. Section III describes the design of the NBI image sensor. Section IV shows the implementation and experimental results. Finally, Section V concludes the work of the wireless NBI capsule endoscope device.

II. Narrowband Image and System Architecture

According to basic physical principles, the penetration depth of light depends on its wavelength. The longer the wavelength is, the deeper the penetration depth it can pierce as depicted in Fig. 1. Based on this, the company Olympus lunched the first endoscope system "EVIS LUCERA SPECTRUM" that offers narrowband imaging [14]. As illustrated in Fig. 2, the system has a xenon lamp and a rotation disk with three NBI filters, instead of RGB optical filters, to allow only three wavelengths to pass through and generate narrowband images. The spectra of the three NBI filters are 415 $\pm$ 30 nm, 445 $\pm$ 30 nm, and 500 $\pm$ 30 nm. A charged-coupled device (CCD) is then used to capture images of these three bands. After that, the NBI image is combined by the video processor using the three-band images. The chice of NBI spectra is based on the light absorption property of hemoglobin. Thus, the microvasculature of the mucosal surface can be clearly seen as dark traces. The longer the wavelength is, the deeper the penetration depth will be. The narrower the light bandwidth, the clearer the developed NBI can be.

For the capsule endoscope application, however, to put a xenon lamp and a rotation disk with three NBI filters into a capsule is hardly possible. Hence, we replaced the xenon lamp and NBI filters with LEDs and color filter array to acquire a narrowband image. The proposed wireless NBI capsule endoscope system is composed of a capsule, a portable data recorder, a real-time monitor, a computer with an image viewer, and a DICOM Gateway, as shown in Fig. 3. The portable data recorder receives an image stream from the RF receiver and saves raw data into flash memory. When recording, the real-time monitor can display the image of the digestive tract for routine examination. After inspection, the received image raw data can be uploaded to a computer through a universal-serial-bus (USB) port. The white-light image (WLI) and narrowband image (NBI) image are then combined and shown by video player software. The DICOM gateway provides a standard for handling, storing, printing, and transmitting information in medical imaging.

Inside the wireless NBI capsule, a narrowband LED light source, a 512 $\times$ 512 dual-mode CMOS image sensor, and an RF transmitter are adopted as illustrated in Fig. 4. Two oxide batteries and an antenna are also installed for power and an RF transmitter. The narrow band-LED light source comprises six LEDs: three white LEDs for WLI and three 430-nm (center wavelength) blue LEDs for narrow NBI. The wireless RF transmitter uses frequency-shift-keying modulation with an 8-Mb/s transmission rate for image data transmitting which operates in the industrial-scientific-medical (ISM) radio band at 416 MHz.

III. Design of the Narrowband CMOS Image Sensor

The acquisition of the narrowband image and reduction of power dissipation are the main challenges of the NBI capsule

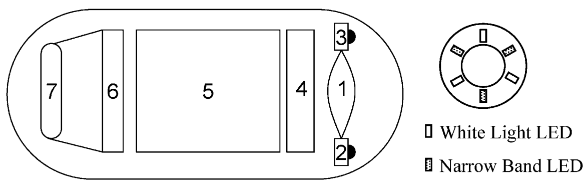

Fig. 4. Structure of the NBI capsule endoscope device: 1) len; 2) blue narrow band LEDs (430 nm); 3) white LEDs; 4) CMOS sensor; 5) battery; 6) RF transmitter; and 7) antenna.

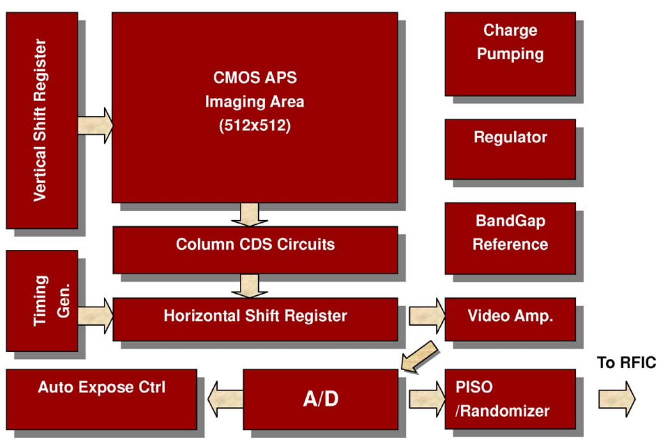

Fig. 5. Block diagram of the CMOS sensor.

endoscope. Fig. 5 shows the block diagram of the CMOS sensor. Each pixel contains three transistors and a photo diode. The charge-pumping circuit produces high voltage for pixel resetting to increase output signal swing. The correlated double sampling circuit is used for low-power noise canceling at the column. The horizontal shift register transfers the sampled charges to a video amplifier. The flash ADC generates a 8-b digital output with very low power consumption. To acquire proper image intensity and decrease the power consumption of LEDs, an autoexpose control application-specific integrated circuit (ASIC) is integrated in the chip. The PISO/randomizer builds an interface between the RF IC and image sensor. The analog and digital circuits inside the chip are powered by the bandgap reference and regulators.

A. Color Filter Array

The color filter array (CFA) is one of the most singular hardware elements in a single monochrome sensor to acquire color information of the image scene [15]. To obtain NBI and WLI on the same sensor, a dedicated color filter array is presented as depicted in Fig. 8. The color filter array acquires the narrowband image on a quincunx grid (B filter and clear pixel N) and the R and G images on rectangular grids. The detail of the color filter spectrum, provided by our manufacturer TSMC, is shown in Fig. 6. According to [1], the difference in narrowband images made by the illumination bandwidth can be emphasized by narrowing the half bandwidth of illumination. The sensitivity spectrum of the clear pixel depends on the illumination spectrum, and the sensitivity spectrum of blue pixel is equal to the spectrum of illumination multiplied by the transmittance of blue CFA as shown in Fig. 7. Thus, the blue pixel and clear pixel can sense the narrow-bandwidth NBI and the

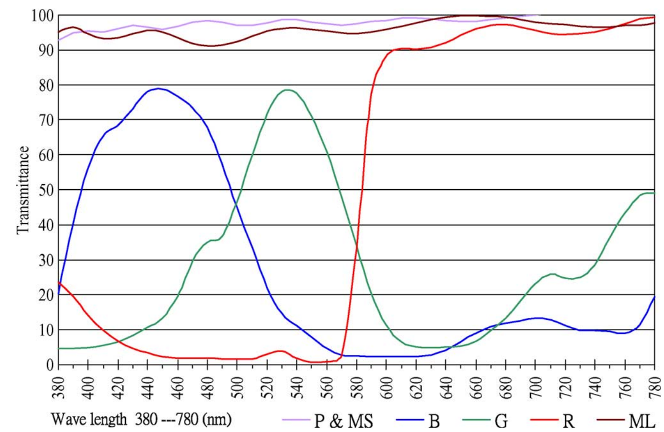

Fig. 6. Center wavelength and spectrum of the R color filter, G color filter, and B color filter.

broad-bandwidth NBI, respectively. When blue LEDs light up, the broad-bandwidth NBI is measured by clear pixel ($\simeq$445 nm) while the narrow-bandwidth NBI is measured by B filter ($\simeq$415 nm). The G filters ($\simeq$540 nm) can provide green color for WLI and NBI when white LEDs turn on. The CMOS sensor can operate in two different illumination modes. In the inter-illumination mode, the white and blue LEDs are turned on frame by frame. At the nth frame, the white LEDs are turned on and we can first acquire R, G, B, and Y (clear pixel) images. In the $(n+1)$th frame, the blue LEDs are turned on, and B pixels and clear pixels (N) are obtained for narrowband image. Accordingly, WLI and NBI images are acquired using RGB and BN patterns, respectively. In intraillumination mode, the white and blue LEDs are turned on in the same frame. The clear pixel is disabled when the white LEDs light up. Hence, the clear pixels contain only narrowband information. By utilizing this arrangement, the NBI image can be established by using the GBN pattern. The CFA allows only one color to be sensed at each location. For computer images, a color image requires three color samples at each pixel at least. This means our sensor must estimate the two missing color values for each pixel for WLI and estimate the missing N and B values for NBI. This estimation process is known as demosaicking. To produce full-scale color and NBI images, the missing components can be estimated from available neighboring components using the CFA demosaicking method.

B. Pixel and Correlated Double-Sampling Circuit

As shown in Fig. 9, each pixel consists of three transistors and a photo diode. The transistor M1 is used to reset the pixel, the transistor M2 acts as a source follower, and the transistor M3 is a row-select transistor with an optical fill factor of 47%. In order to increase the output voltage swing under low power supply, a higher voltage pulse driven by the charge-pumping circuit is used to reset the photo diode. Since the responsivity of pixels varies with the variation in manufacturing, the CMOS sensor will have spatial noise, called fixed pattern noise (FPN). The correlated double sampling circuit in each column can efficiently diminish the column fixed pattern noise, caused by V_t variation of the source follower transistor, by two sample-hold capacitor C1 and C2. Fig. 9 also shows the timing diagram of

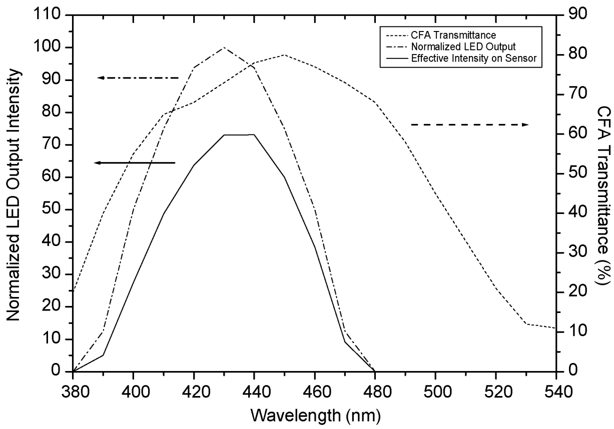

Fig. 7. Effective sensitivity spectrum of the clear pixel (dash-dot line) and blue pixel (solid line).

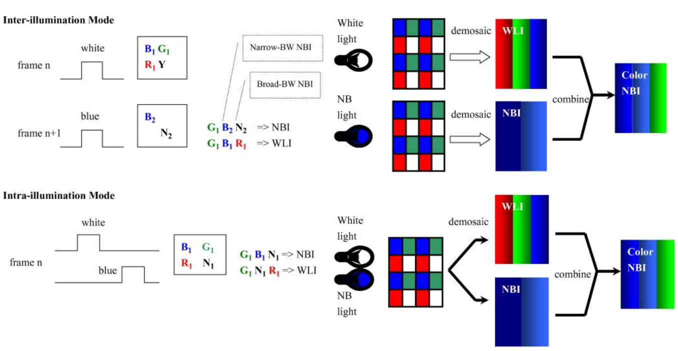

Fig. 8. Sensor illumination modes.

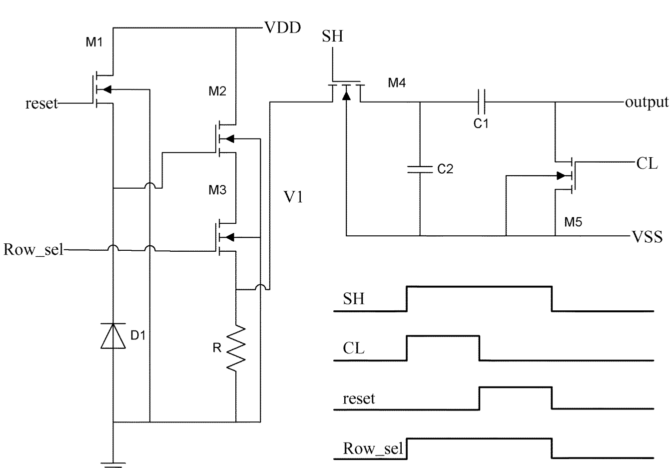

Fig. 9. Timing diagram of pixel reset and CDS operations.

pixel reset and CDS. When the pass transistor M3 and M4 are ON, C1 and C2 are both charged to V1. As the pass transistor M5 is OFF and M1 is ON, C2 is charged to Vreset. When M3 and M4 are OFF, the output voltage will rise to (Vreset-V1). Since each pixel at the same column passes through an identical CDS circuit and the output sensing voltage is double sampled, the FPN caused in the column direction will be removed. Transistor M2 acts as a source follower.

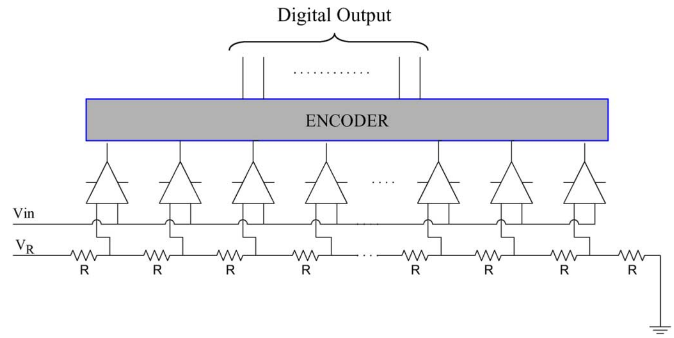

Fig. 10. Equivalent block diagram of the 8-b flash ADC.

C. ADC

Fig. 10 shows the equivalent block diagram of the 8-b flash analog-to-digital converter (ADC) used in the CMOS sensor. It is composed of 127 comparators, a resistor network, and an encoder. The resistor network methodizes the input between two neighboring comparators equal to one least-significant bit (LSB). In actual circuits, the 8-b ADC was built by cascading sixteen 4-b ADCs. The encoder converts thermal code that is the output of 127 comparators to binary code. Inside the comparator, the L/W ratio of transistors should also be as large as possible to avoid the mismatching problem of comparators under low reference voltage V_R. Although the flash ADC is suitable for high-speed video application, the circuit consumes considerable power and suffers from babbling and metastable effects. To overcome these drawbacks, it is necessary to decrease the power consumption of comparators. Inside the comparator, the power dissipation will be dramatically reduced by increasing the active load of differential pairs at the expense of the throughput rate of the ADC. In the proposed NBI wireless capsule endoscope, the CMOS sensor works at 2 frames/s. The requirement of the ADC throughput rate is as low as 1 MHz. Thus, the expense of the throughput rate is affordable in our paper.

D. Auto Expose Control Digital Circuit

The white and blue LEDs in the proposed NBI wireless capsule endoscope behave as a strobe light source for WLI and NBI images capturing. During the routine capsule endoscope examination, the appearances of the gastrointestinal tract may be changed dramatically. To acquire high-contrast images and decrease power consumption of LEDs, an auto expose control ASIC is implemented by adjusting the strobe pulsewidth of LEDs. The algorithm for strobe pulsewidth modulation is shown in (1), which is achieved by histogram processing. The resolution of the strobe pulse width is the half horizontal line time

$$pw_s = \begin{cases} pw_s + 1, & \text{if} \quad h\left(r_u(x,y)\right) > n_s \times 0.2 \\ pw_s - 1, & \text{else if} \quad h\left(r_d(x,y)\right) < n_s \times 0.2 \\ pw_s, & \text{otherwise} \end{cases} \tag{1}$$

where $h(r_u)$ is the number of pixels with a gray level in coordinate (x, y) greater than r_u, while $h(r_d)$ is the number of pixels

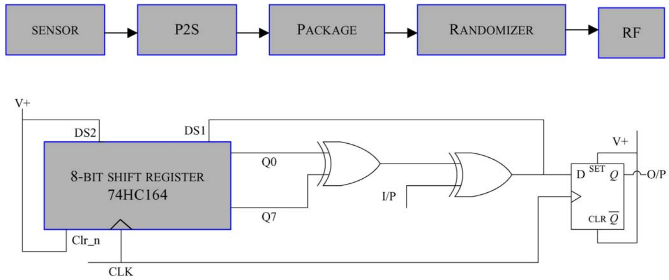

Fig. 11. Data flow and schematics of the randomizer.

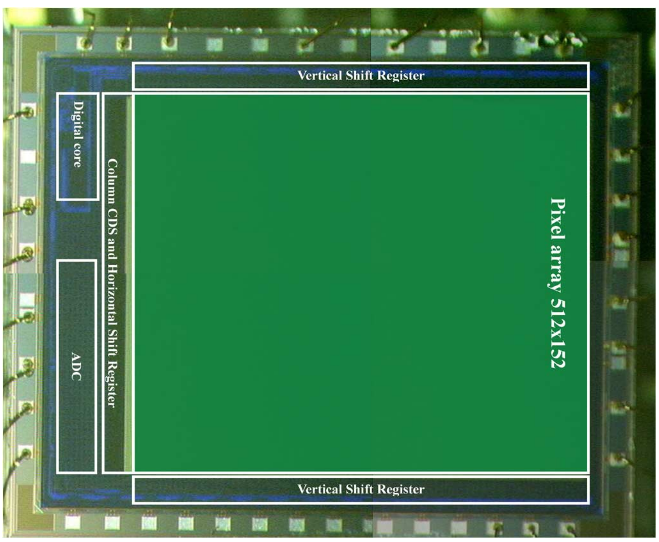

Fig. 12. Chip photomicrograph.

TABLE I
CHIP SPECIFICATIONS

Technology	0.25μm 1P4M CMOS
Chip Size	3.7mm x 3.95mm
Format	512x512
Pixel size	5.6μmx5.6μm
Fill Factor	47%
ADC resolution	8bit
Frame rate	2Hz
Power Consumption	2mA@3V

TABLE II
SPECIFICATIONS OF POWER CONSUMPTION

Circuit Block	Current@3V
8 bit ADC	0.5mA
Pixel Circuit	0.077mA
Column CDS Circuit	0.12mA
VideoAmp.	0.5mA
BandGap Reference	0.025mA
Regulator	0.04mA
Digital Core	0.03mA@2.5V

with gray level in coordinate (x, y) greater than r_d, n_s indicates the total number of pixels in B and N for blue LEDs or R and G for white LEDs, s indicates the strobe pulsewidth for white or blue LEDs, (x, y) is the coordinate of B and clear pixel N in NBI or G and R in WLI.

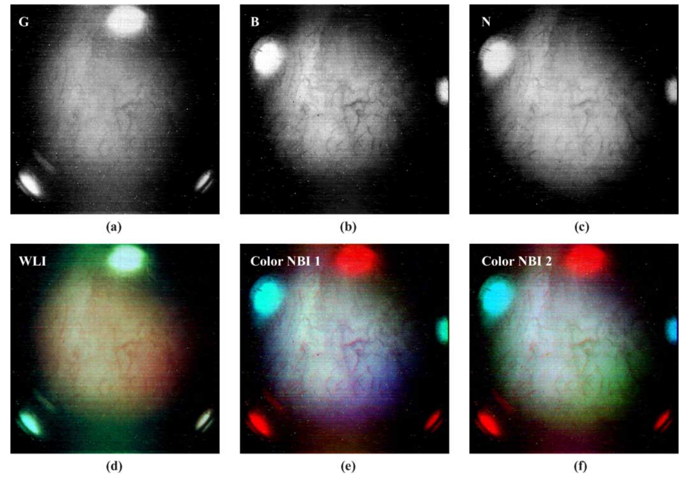

Fig. 13. (a) Demosaicked images of the green pixel. (b) The demosaicked images of the blue pixel. (c) The demosaicked images of clear pixels. (d) The WLI image. (e) The first-type color NBI. (f) The second-type color NBI of the backside mucosa of the human tongue.

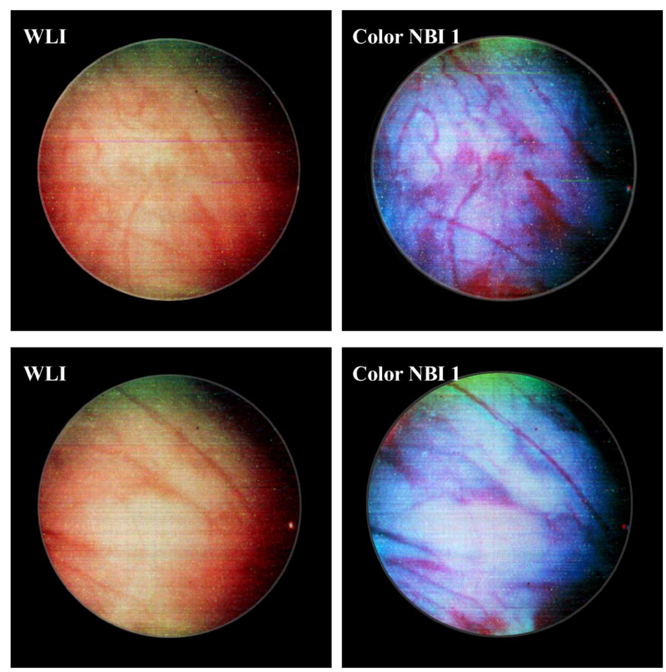

Fig. 14. WLI and combined color NBI of the live pig's duodenum in interillumination mode.

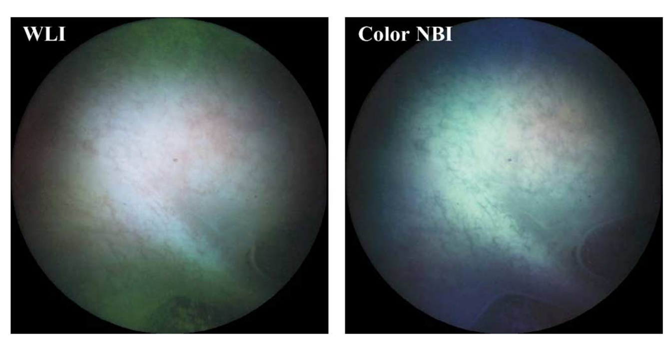

Fig. 15. WLI and combined color NBI images of backside mucosa of the human tongue in intraillumination mode.

With the help of an autoexpose control ASIC, the expose time of the CMOS sensor can be reduced when the acquiring image is saturated. In other words, lower duty cycle of the strobe pulsewidth lead to reducing the energy dissipation of LEDs.

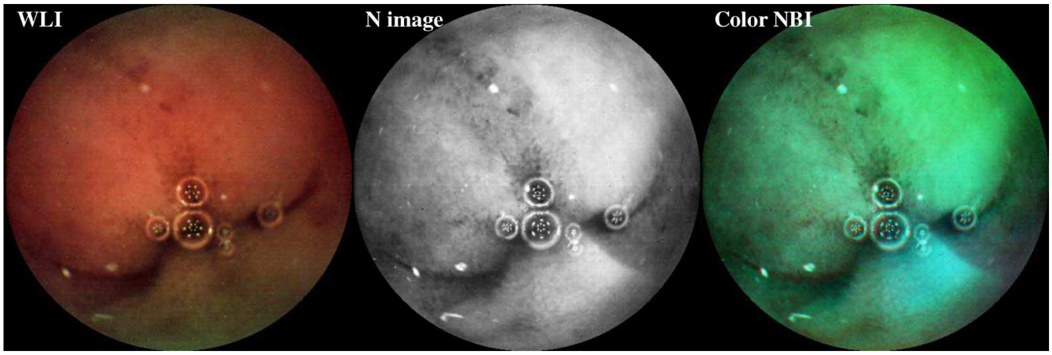

Fig. 16. Small bowel of the life pig shown in WLI, gray narrowband image, and color NBI.

E. Randomizer

The parallel digital image signal after P/S is modulated by the randomizer. The randomizer guarantees the RF IC to transmit the serial binary data stream without continual "0" or "1," as illustrated in Fig. 11. The serial binary data stream from P/S is applied to the I/P of the second XOR gate.The 8-b shift register and the first XOR gate randomize the serial binary data stream and the output is given to the other input of second XOR gate. In order to eliminate the glitch of O/P and obtain a 50% duty cycle square wave, a D flip-flop is added.

IV. Implementation and Experiment Results

A. NBI CMOS Image Sensor

The dual-mode CMOS image sensor is fabricated in 0.25-μm single-poly four-metal CMOS technology with an area of 3.7 mm $\times$ 3.95 mm. It consumes 2 mA at 2 frames/s with a 3-V power supply while the analog-to-digital converter (ADC) and video amplifier waste 0.5 mA individually. Fig. 12 shows a photomicrograph of the image sensor. The timing generator, P/S, randomizer, and auto expose control circuit are all integrated into the digital core. The specifications are summarized in Table I. Detailed specifications of power consumption are described in Table II. Fig. 13 illustrates demosaicked and combined images of a backside mucosa of a human tongue by using the dedicated CMOS image sensor at 2 frames/s in interillumination mode. In this experiment, the image data stream is transmitted by the conduction line and been demodulated to reconstruct the raw image. After using the bilinear CFA demosaicking method [16], the first-type color NBI image Fig. 13(e) is combined by assigning the previous G image to red plane, N and B images to blue and green plane, while the second-type color NBI image Fig. 13(f) is combined by assigning the previous G image to the red plane, as well as N and B images to the green and blue plane. This demonstrates that the designed CMOS sensor provides a white light image Fig. 13(f) and enhanced color NBI images. Fig. 14 provides another image of the live pig's duodenum by the NBI capsule endoscope prototype. Fine vascular patterns can be easily identified by color NBI when compared to WLI.

Fig. 15 shows the acquired images when the sensor works in intraillumination mode. Although the color of the WLI image is slightly distorted, because the G and R image is influenced by narrowband LEDs, the WLI and NBI are still distinguishable and the captured images are doubled.

B. NBI Capsule Endoscope Prototype

A wireless NBI capsule endoscope system that has been described in Section II is developed. Due to a limited print-circuit board (PCB) area, the sensor and RFIC are bound to the PCB by chip-on-board (COB) technology. Other on-board components, such as resistors and capacitors, are used with the surface-mount-device (SMD) package. As shown in Fig. 17, the narrowband LED module, wide FOV lens, dual-mode NBI CMOS sensor, batteries, RF transmitter, magnetic switch, and antenna are all capsuled into a pill. The RF receiver dissipates less than 0.5 A at 5 V while the sensitivity is lower than -80 dBm. The data recorder can store more than 4 GB and meantime the image viewer displays the received images through the USB port. The average current of the capsule is nearly 7 $\sim$ 8 mA when the RF transmitter works at 8 Mb/s and the sensor works at 2 frames/s. With two 1.5-V 80-mAh silver–oxide button batteries, experiments show that the capsule continues working for 6 $\sim$ 8 h.

C. Experiment on Animal

As shown in Fig. 18, to demonstrate the proposed wireless NBI capsule endoscope, we deposit the capsule into a pig's duodenum directly by a surgical operation since the digestive time of a pig is nearly two weeks. The CMOS sensor is setting to interillumination mode. Fig. 16 provides the images of a pig's small bowel in the experiment. As we can see in Fig. 16, the pile of small bowel in the WLI images is revealed clearly, but the gray narrowband images (N images), composed of clear and blue pixel, can show more details on the pile. By combining the G plane of WLI and gray N image, the color NBI clearly demonstrates the features of the small intestine that could not be seen by WLI and gray N image observations. These results imply that the NBI capsule endoscope might offer a breakthrough in the field of gastrointestinal tract diagnosis.

V. Conclusion

In this paper, a novel narrowband imaging capsule endoscope is presented. Compared with a standard wireless capsule endoscope, the dedicated dual-mode 512 $\times$ 512 CMOS sensor in the NBI capsule can offer WLI and NBI images by comprehending the optical properties of tissue and controlling the illumination wavelength and procedure. For the sake of power,

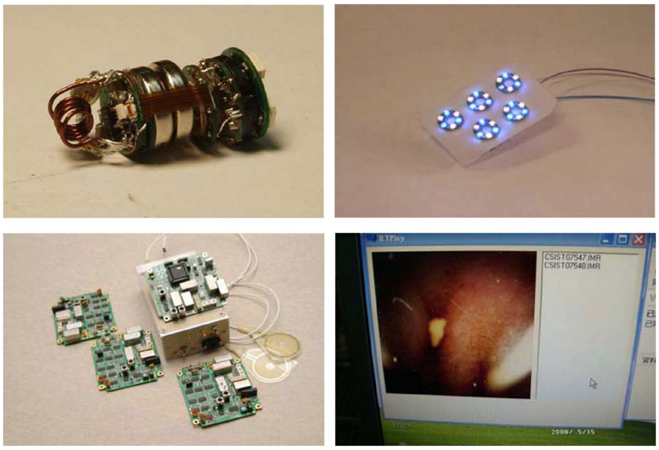

Fig. 17. NBI capsule endoscope (top left: NBI capsule endoscope; top right: LED module; bottom left: receiver and data recorder; bottom right: image viewer).

Fig. 18. Experiment on an animal.

effective low-power techniques need to be utilized in the design to guarantee long working time. With a 3-V power supply, implementation results show the sensor consumes only 2 mA at 2 frames/s and the entire wireless NBI capsule that dissipates nearly $7 \sim 8$ mA can work for $6 \sim 8$ h consecutively. Experiment results on the backside mucosa of a human tongue and pig's small intestine demonstrate that the NBI capsule endoscope is a beneficial tool for discriminative diagnosis by providing a contrast-enhanced image of vascular and white light image.

Acknowledgment

The authors would like to thank Dr. S.-M. Wu and Dr. P.-K. Weng for their technical support.

References

[1] K. Gono, "Multifunctional endoscopic imaging system for support of early cancer diagnosis," *IEEE J. Sel. Topics Quant. Electron,*, vol. 14, no. 1, pp. 62–69, Jan./Feb. 2008.

[2] K. Gono, T. Obi, M. Yamaguchi, N. Ohyama, H. Machida, Y. Sano, S. Yoshida, Y. Hamamoto, and T. Endo, "Appearance of enhanced tissue features in narrowband endoscopic imaging," *J. Biomed. Opt.*, vol. 9, p. 568V577, May/Jun. 2004.

[3] K. Gono, K. Yamazaki, N. Doguchi, T. Nonami, T. Obi, M. Yamagichi, N. Ohyama, H. Machida, Y. Saono, S. Yoshida, Y. Hamamoto, and T. Endo, "Endoscopic observation of tissue by narrowband illumination," *Opt. Rev.*, vol. 10, p. 211V215, 2003.

[4] M. Muto, C. Katada, Y. Sano, and S. Yoshida, "Narrow band imaging: A new diagnostic approach to visualize angiogenesis in superficial neoplasia," *Clin. Gastroent.. Hepatol.*, vol. 3, no. 7, pp. 3:S16–3:S20, 2005.

[5] P. Sharma, "Narrow band imaging in barrett's esophagus," *Clin. Gastroent. Hepatol.*, vol. 3, no. 7, pp. 3:S21–3:S22, 2005.

[6] G. Iddan, G. Meron, A. Glukhovsky, and P. Swain, "Wireless capsule endoscopy," *Nature*, vol. 405, pp. 417–418, May 25, 2000.

[7] X. Chen, X. Zhang, L. Zhang, X. Li, N. Qi, H. Jiang, and Z. Wang, "A wireless capsule endoscope system with low-power controlling and processing asic," *IEEE Trans. Biomed. Syst.*, vol. 3, no. 1, pp. 11–22, Feb. 2009.

[8] X. Xie, G. Li, X. Chen, X. Li, and Z. Wang, "A low-power digital ic design inside the wireless endoscopic capsule," *IEEE J. Solid-State Circuits*, vol. 41, no. 11, pp. 2390–2400, Nov. 2006.

[9] M.-C. Lin, L.-R. Dung, and P.-K. Weng, "A cardinal image compression for capsule endoscope," presented at the IEEE Biomedical Circuits and Systems Conf., London, U.K., 2006.

[10] L.-R. Dung, Y.-Y. Wu, H.-C. Lai, and P.-K. Weng, "A modified h.264 intra-frame video encoder for capsule endoscope," presented at the IEEE Biomedical Circuits Systems Conf., Baltimore, MD, 2008.

[11] J. Macdonald, V. Porter, and D. McNamara, "Negative capsule endoscopy in patients with obscure gi bleeding predicts low rebleeding rates," *Gastrointest. Endoscopy*, vol. 68, no. 6, pp. 1122–1127, 2008.

[12] L. H. Lai, "Obscure gi bleeding: Is capsule endoscopy sufficient?," *Gastrointest. Endoscopy*, vol. 68, no. 6, pp. 1128–1130, 2008.

[13] L.-R. Dung, Y.-Y. Wu, and P.-K. Weng, "A wireless narrow-band imaging chip for capsule endoscope," presented at the IEEE Biomedical Circuits and Systems Conf., Beijing, China, 2009.

[14] Olympus launches EVIS Lucera Spectrum Video Imaging System for NBI support for normal light imaging and narrow band imaging (NBI). Olympus. [Online]. Available: http://www.olympus-europa.com

[15] R. Lukac and K. N. Plataniotis, "Color filter arrays: Design and performance analysis," *IEEE Trans. Consum. Electron.*, vol. 51, no. 4, pp. 1260–1267, Nov. 2005.

[16] B. K. Gunturk, J. Glotzbach, Y. Altunbasak, R. W. Schafer, and R. M. Mersereau, "Demosaicking: Color filter array interpolation," *IEEE Signal Process. Mag.*, vol. 22, no. 1, Jan. 2005.

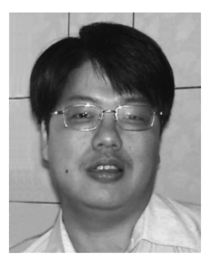

Lan-Rong Dung (SM'93–M'97) received the B.S.E.E. degree from Feng Chia University, Taiwan, in 1988, the M.S. degree in electronics engineering from National Chiao Tung University, Hsinchu, Taiwan, in 1990, and the Ph.D. degree in electrical and computer engineering from the Georgia Institute of Technology, Atlanta, in 1997.

From 1997 to 1999, he was with Rockwell Science Center, Thousand Oaks, CA, as a member of the Technical Staff. He joined the faculty of National Chiao Tung University, Taiwan, in 1999, where he is currently an Associate Professor in the Department of Electrical and Control Engineering. His current research interests include very-large scale integrated design, digital signal processing, hardware-software codesign, and system-on-a-chip architecture.

Prof. Dung received the Best Student Award from Feng Chia University, Taiwan, in 1988. He received the VHDL International Outstanding Dissertation Award Celebration in Washington, DC, in 1997. He is a member of IEEE Circuits and Systems and Signal Processing societies.

Yin-Yi Wu received the M.S. degree in electronic and information from National Yunlin University of Science and Technology, Taiwan, in 1999, and is currently pursuing the Ph.D. degree in electrical engineering at National Chiao Tung University, Hsinchu, Taiwan.

He then joined the Materials and Electro-Optics Division, Chung-Shan Institute of Science and Technology. His current interests include integrated-circuit design and image processing.